AGU ADVANCING EARTH AND SPACE SCIENCE

Geophysical Research Letters

Key Points:
- The modern Limpopo River of South Africa formed in the Plio-Pleistocene
- Plio-Pleistocene drainage reorganization was driven by climate change
- Formation age and driving mechanisms of South African rivers are revisited

Correspondence to:
J. Nie and X. Hu,
jnie@lzu.edu.cn;
feixhu@lzu.edu.cn

Climatic Forcing of Plio-Pleistocene Formation of the Modern Limpopo River, South Africa

Jing Yang[1], Junsheng Nie[1,2], Eduardo Garzanti[3], Mara Limonta[3], Sergio Andò[3], Pieter Vermeesch[4], Haobo Zhang[1], Xiaofei Hu[1], Zhao Wang[5], Baojin Zhao[6], Lindani Ncube[6], Thomas Stevens[7], Maotong Li[1], Hua Li[8], Taian Chen[1], Yunfa Miao[9], and Baotian Pan[1]

[1]Key Laboratory of Western China's Environmental Systems (Ministry of Education) College of Earth and Environmental Sciences, Lanzhou University, Lanzhou, China, [2]CAS Center for Excellence in Tibetan Plateau Earth Sciences, Chinese Academy of Sciences (CAS), Beijing, China, [3]Department of Earth and Environmental Sciences, Laboratory for Provenance Studies, University of Milano-Bicocca, Milano, Italy, [4]Department of Earth Sciences, University College London, London, UK, [5]College of Geographical Sciences, Shanxi Normal University, Taiyuan, China, [6]Department of Environmental Sciences, University of South Africa, Florida, South Africa, [7]Department of Earth Sciences, Uppsala University, Uppsala, Sweden, [8]School of Materials and Energy, Lanzhou University, Lanzhou, China, [9]Northwest Institute of Eco-Environment and Resources, Chinese Academy of Sciences, Lanzhou, China

Abstract Understanding the evolution of river systems in southern Africa is fundamental to constrain the evolution of landscape and sediment dispersal patterns. It is widely considered that the upper Zambezi River was connected with the Limpopo River during the Cretaceous, forming what was then the largest river in Africa. Crustal flexure during the Paleogene severed the upper Zambezi drainage from the Limpopo, setting the framework of the modern Zambezi and Limpopo River systems. We present first evidence—based on heavy-mineral assemblages from cores drilled offshore of the Limpopo River mouth and samples collected in different reaches of the modern Limpopo River, integrated with magnetic susceptibility, detrital-zircon geochronology, and geomorphological analysis—suggesting that the current Limpopo River formed recently in the Plio-Quaternary. Plio-Quaternary climate change is envisaged to have controlled the recent dynamics of river drainage and consequent distribution of sediment loads, as observed in many other transcontinental rivers worldwide.

Plain Language Summary Landscape evolution, sediment dispersal patterns, and the accumulation of hydrocarbon and mineral resources in southern Africa, were largely determined by the evolution of the vast Zambezi-Limpopo River system. It is widely believed that this river system attained its current configuration during the late Paleogene as a consequence of mantle-driven dynamic uplift. Based on heavy-mineral assemblages from river sediments and an International Ocean Discovery Program ocean core, we argue here instead for a Plio-Pleistocene age for the formation of the modern characteristics of the Limpopo River (i.e., tens of millions of years younger than previously thought). This challenges the current paradigm on both formation modality and driving mechanisms of this vast river system. Plio-Pleistocene climate change is envisaged to have controlled the dynamics of river drainage and consequent distribution of sediment loads, as observed in several other transcontinental rivers worldwide, underscoring the importance of these climate changes in driving river evolution world-wide.

1. Introduction

Large river systems play a key role in shaping the Earth's landscape. Drainage is strongly affected by climate change and, in turn, rivers contribute to modifying global climate by transferring large amounts of terrestrial inorganic and organic carbon to the ocean, where it remains buried for long periods, thus impacting the carbon cycle (Galy et al., 2007; Zheng et al., 2013). However, because of the complex and interacting roles of tectonic versus climatic forcing on river erosion, the origin and history of large river systems is difficult to constrain (Blum et al., 2018; Craddock et al., 2010; Nie et al., 2015). In Asia, the Yellow River draining the northeastern Tibetan Plateau originated during the Plio-Pleistocene (Z. Wang et al., 2019), often interpreted as an effect of intensified monsoon precipitation and decreased evaporation, resulting in lake spill-over and expansion of the drainage area (Craddock et al., 2010). Plio-Pleistocene uplift of the Tibetan Plateau,

however, likely also contributed (Li et al., 2014) and this example highlights the difficulties in untangling interplaying controls especially in compressional tectonic settings. Studying transcontinental rivers draining cratonic continental blocks minimizes the difficulty associated with the complex tectonic evolution of orogens and thus facilitates a more accurate assessment of the role played by climate in the formation and evolution of drainage.

During the Cretaceous-Paleogene, the coupled Zambezi-Limpopo River system represented the largest fluvial system in Africa (Du Toit, 1927; Moore & Larkin, 2001). Understanding how it evolved through time across the changing landscapes of southern Africa is essential to reconstruct the pattern of dispersal and distribution of sediment generated within its vast catchment, as well as the concentration of mineral resources (de Wit, 1999; Key et al., 2015; Moore & Blenkinsop, 2002; Moucha & Forte, 2011; van der Beek et al., 2002; Walford et al., 2005).

Southern Africa is characterized by the steep Great Escarpment, inherited from domal uplift that preceded the late Mesozoic opening of the Indian and South Atlantic Oceans (Cox, 1989). The Great Escarpment encircles the slowly denudating southern African Plateau, lying at a mean elevation of ∼1,000 m a.s.l. (Flowers & Schoene, 2010). Although the modern Limpopo is smaller than the Zambezi, geomorphological evidence has long been used to suggest that the upper Zambezi was a tributary of the Limpopo until the Oligocene, when uplift of the Ovambo-Kalahari-Zimbabwe axis severed the link between the two rivers and set the framework for the independent development of the Zambezi throughout the Neogene (Du Toit, 1927; Moore & Larkin, 2001, Figure 1a). According to this scenario, the Limpopo River has a long history and the current valley is inherited from its ancestral river established at least 125–130 Ma, at the time of rift-shoulder uplift associated with incipient opening of the South Atlantic Ocean (Key et al., 2015; Moore & Larkin, 2001). Distinct phases of accelerated erosion took place in the Zambezi-Limpopo watershed during the Early Cretaceous, Late Cretaceous, and Paleogene (Braun et al., 2014; Flowers & Schoene, 2010). No major tectonic uplift has been documented during the Plio-Quaternary (Moore et al., 2009), although this is known to be a period of major climate change (Lisiecki & Raymo, 2005; Zhang et al., 2001). Therefore, the evolution of the Limpopo River represents an ideal case for testing the role played by climate in shaping river drainage. The proposed mechanisms for southern African landscape evolution and river formation vary from mantle-controlled (Burke, 1996) to plate tectonics-controlled (Moore et al., 2009) and also climate-controlled (Braun et al., 2014). In this article, we investigate the recent dynamics of the Limpopo River primarily by applying heavy-mineral analysis of sediments deposited offshore of the river mouth and drilled during the International Ocean Discovery Program (IODP) Expedition 361 and geomorphological analysis based on χ values. These data are used to constrain sediment provenance as well as the timing and relative roles played by different geological processes such as dynamic uplift, extensional tectonics, and climate change on the drainage evolution in southern Africa.

2. Materials and Methods

Heavy minerals are widely used as tracers of sediment provenance. In this study, we analyzed the heavy minerals separated from 18 samples of marine sediments from IODP Expedition 361 Site U1478A (25°49.26′S; 34°46.14′E; water depth 488 m; Figure 1). Core samples were collected in the depth range 0–248 m b.s.f. (below seafloor) (Figure S1), corresponding to depositional ages between 0 and 4.05 Ma according to the orbitally tuned age-model for Site U1478 (Koutsodendris et al., 2021). For comparison, we also show previously the published heavy-mineral data from six modern samples (Hahn et al., 2018): #34 from the Incomati River, #37 from a floodplain lake in the lower Limpopo Valley, #36 from the Changane River (a lower Limpopo tributary), #40 and #41 from the middle Limpopo mainstem, #44 from the Olifants River (a main tributary of the Limpopo River), and #48 from the upper Limpopo mainstem.

The Site U1478A samples were wet sieved with a standard 500 μm steel sieve and with hand-made nylon sieves with 15 or 5 μm mesh. Heavy minerals were separated from the 5–500 μm or 15–500 μm fraction by centrifuging in Na polytungstate (density 2.90 g/cm³). The same procedure was followed for the treatment of modern terrestrial sediments reported in Hahn et al. (2018) and both sets of samples were analyzed in the Laboratory for Provenance Studies, Department of Earth and Environmental Sciences, University of Milano-Bicocca. On each grain mount, ≥200 transparent heavy minerals were point-counted under
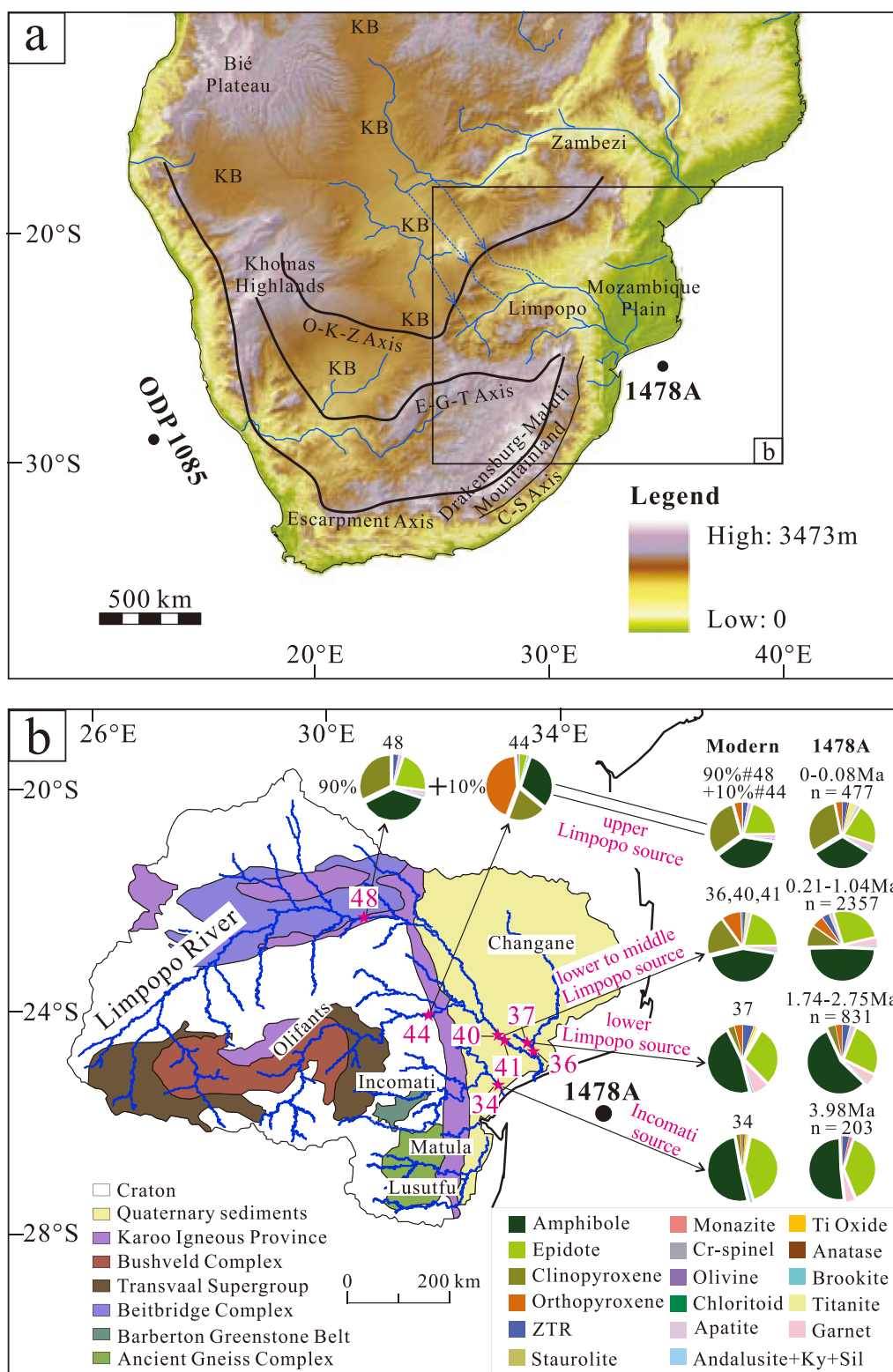
Figure 1

a polarizing microscope to obtain real volume percentages (Garzanti & Andò, 2019). All dubious grains were analyzed using Raman spectroscopy (Andò & Garzanti, 2014). To visualize the comparison between terrestrial and IODP samples, we performed Correspondence analysis (CA) on the heavy-mineral data (Vermeesch, 2018). CA is a multivariate ordination technique similar to principal component analysis (PCA) but specifically tailored to categorical rather than continuous data (Greenacre, 1984; Vermeesch, 2018). It treats the data as compositions without requiring the logratio transformation that is customary in compositional PCA (Aitchison, 1983). CA is immune to the zero-count problem that plagues compositional PCA, and CA achieves this by using chi-square distances instead of Euclidean distances to compare the samples (Vermeesch, 2018). Like PCA, CA results are best visualized as biplots (Aitchison & Greenacre, 2002), which encode information about both the samples and the variables. However, when interpreting these plots, it is important to bear in mind that the CA scores are based also on rare minerals that are subject to random counting uncertainty. The diagram is thus useful to visualize data and discern general trends but should not be used as the sole basis for provenance interpretation of individual samples.

We also tried to separate zircons from the same samples from which we generated heavy mineral data. Due to the small size of cored samples and fine grain size, only the U1478A core-top sample yielded enough zircons for U-Pb dating. For detailed analysis method, please see Text S1.

In addition to heavy-mineral and zircon U-Pb ages analyses, we utilize the parameter χ representing the relative gradient of the longitudinal profile of a river to determine whether a river network is in equilibrium on both sides of a drainage divide (similar χ) or not (Perron & Royden, 2013). In the latter case, the drainage divide moves in the direction of higher χ to achieve equilibrium (Willett et al., 2014). In this study, we used the American Shuttle Radar Topography Misson 90-m-resolution Digital Elevation Model (https://srtm.csi.cgiar.org/), using ArcGIS and MATLAB to calculate χ and determine the equilibrium state of river networks on both sides of the Limpopo River drainage divide (Text S2).

3. Results and Interpretation

Heavy-mineral data from Site U1478A allow us to identify four distinctive intervals corresponding to dated stratigraphic intervals: 3.98, 2.75–1.74, 1.04–0.21, and 0.08–0 Ma (Figure 1b). The heavy-mineral composition of the single Pliocene sample (3.98 Ma) is similar to the modern Incomati River rather than to any modern Limpopo River samples currently available (Figures 2e and 2f). Amphibole and epidote in roughly equal proportions account together for over 95% of the transparent heavy-mineral population. In contrast, samples from the 2.75 to 1.74 Ma interval have a smaller proportion of epidote and they contain pyroxene (Figure 1b). This heavy-mineral assemblage is similar to that of lacustrine sample #37 from the lower reaches of the Limpopo catchment (Hahn et al., 2018). Samples deposited in the 1.04–0.21 Ma interval can be divided into two categories. Those deposited at 0.87, 0.54, 0.52, 0.31, and 0.21 Ma have a transparent-heavy-mineral suite similar to sample #37, representing the lower reach signal, whereas the rest of the samples are similar to samples #40 and #41 of the middle reach Limpopo main channel and to sample #36 from its Changane branch (Figures 2e and 2f). Clinopyroxene increases in the sample deposited at 0.08 Ma, where it represents the most common heavy mineral, reaching a percentage similar to modern upper Limpopo sediments (sample #48; Figures 2e and 2f). The heavy-mineral signature of all these samples points to provenance from the lower to middle reaches of the present Limpopo catchment.

The U1478 core top sample's zircon U-Pb age spectrum shows a highest peak at 2.6–2.7 Ga, a Neoarchean age typical of rocks in the Limpopo Belt and Zimbabwe and Kaapvaal Cratons (Figure S2; Garzanti et al., 2014), consistent with the upper reaches as the dominant source for modern Limpopo River sand (Figure 1b). However, this spectrum exhibits multiple peaks, suggesting contribution from diverse other sources. A second-highest peak is observed at 2.0–2.1 Ga, which is sourced chiefly from the Olifants River catchment

Figure 1. Geological and geomorphological map of the study area showing heavy-mineral assemblages of Limpopo River sediment samples. (a) Shuttle Radar Topography Misson digital elevation image and drainage system of southern Africa. E-G-T, Etosha-Griqualand-Transvaal Axis; O-K-Z, Ovambo-Kalahari-Zimbabwe Axis; C-S, Ciskei-Swaziland Axis; KB, Kalahari Basin. The blue dotted lines represent the hypothesized river courses connecting the upper Zambezi and Limpopo Rivers (Moore et al., 2009; Spaliviero et al., 2014). (b) Limpopo drainage area, geology (Schüürman et al., 2019), and sampling sites. Heavy-mineral composition of modern sediments (Hahn et al., 2018) and sediments cored at International Ocean Discovery Program Site U1478A, along with age and inferred source region, are shown by pie charts. Ky, Kyanite; Sil, Sillimanite.
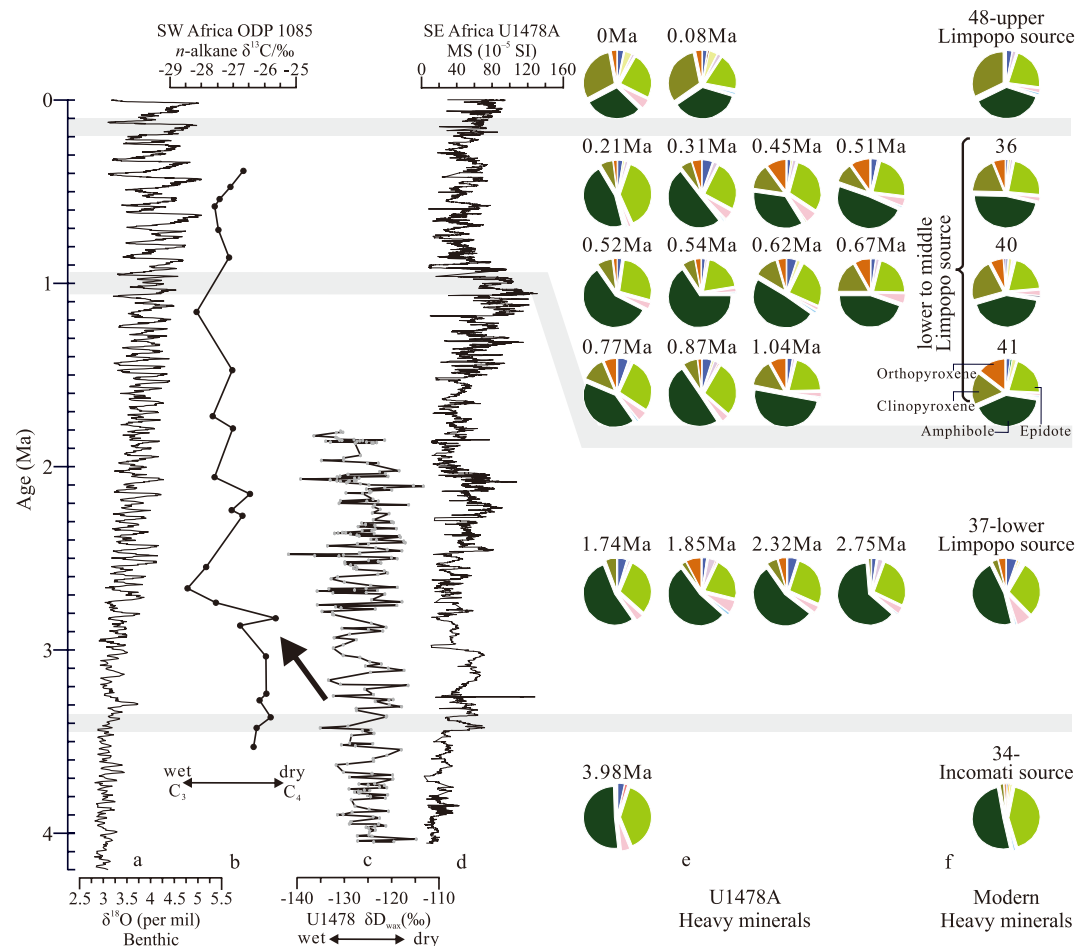
Figure 2. Comparison of heavy-mineral suites from sediments cored at International Ocean Discovery Program (IODP) Site U1478A with different reaches of the Limpopo River and paleoclimate records. (a) Benthic $\delta^{18}O$ stack record (Lisiecki & Raymo, 2005). (b) Southwest (SW) Africa ODP Site U1085 n-alkane $\delta^{13}C$ values (Maslin et al., 2012). (c) Southeast (SE) Africa IODP Site U1478 δD_{wax} values (Taylor et al., 2021). (d) Whole-round core magnetic susceptibility (MS) in Hole U1478A (Hall et al., 2017). (e) The heavy-mineral data from Hole U1478A (this study). (f) The heavy-mineral data from modern sediments (Hahn et al., 2018). Color indices for different minerals are the same as in Figure 1.

(Figure S2; Garzanti et al., 2014). This suggests that the Olifants contributed sediments to the drill site back to 0.08 Ma. Another fingerprint of the Olifants River is the abundance of orthopyroxene, which is lacking in Upper Limpopo sample #48 but present in small quantities (∼3%) in drill core samples deposited at 0.08 and 0 Ma, suggesting minor contribution from the Olifants River (Figure 1b). The CA biplot of the heavy mineral data are broadly consistent with these provenance inferences (Figure 3; Text S3).

The χ value distribution pattern demonstrates that the Limpopo River is not in equilibrium, with χ exhibiting lower values to the west of its drainage divides (Figure 4).

4. Discussion

Provenance analysis based on multiple techniques is the best approach in tracing sediment sources and pathways (Garzanti, 2016; Jonell et al., 2017; Nie et al., 2012). In order to test the validity of the recognized provenance changes based on heavy minerals, we used recently published magnetic susceptibility data from the same sediment core (Hall et al., 2017).

Different sediment source regions are expected to yield different combinations and concentrations of magnetic minerals. These differences can result in different magnetic properties in sediments derived from
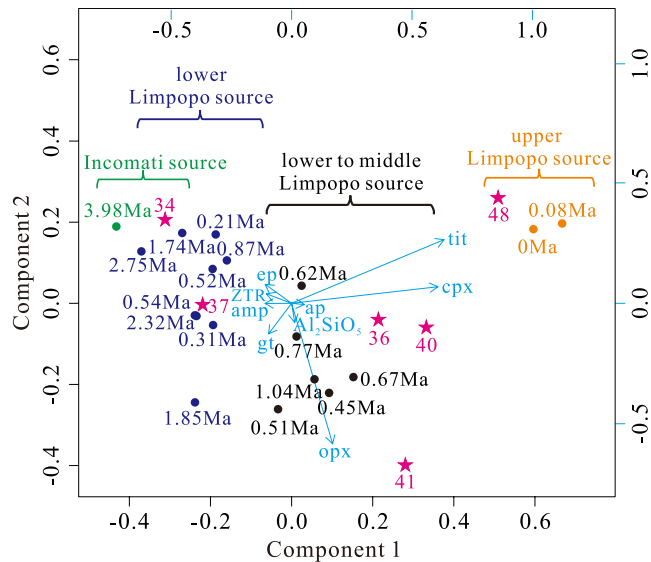
Figure 3. Correspondence analysis (CA) biplot (Vermeesch, 2018) of the heavy-mineral data, produced using the "provenance" R package (Vermeesch et al., 2016). Marine and terrestrial samples are shown in dots and stars, respectively. Al$_2$SiO$_5$, andalusite + sillimanite + kyanite; amp, amphibole; ap, apatite; cpx, clinopyroxene; ep, epidote; gt, garnet; opx, orthopyroxene; tit, titanite; ZTR, zircon + tourmaline + rutile.

different source regions, which reflect the distribution of source rocks in different catchments (Hällberg et al., 2020; Maher, 2011). The exposed basement of the Limpopo upper to middle reaches is mainly gneissic with subordinate mafic complexes and volcanic rocks, whereas sedimentary strata are dominant in the lower reaches (Schüürman et al., 2019). By contrast, mainly greenstone belts are exposed in the Incomati River catchment (Schüürman et al., 2019). These differences affect both the magnetic and non-magnetic heavy minerals generated in these catchments. Heavy-mineral suites and magnetic susceptibility of sediments combined should thus reflect the different distribution of source rocks in different parts of the Limpopo catchment.

The provenance shifts recorded by heavy-mineral data (Figures 2e and 2f) are consistent with changes in the high-resolution magnetic susceptibility data set (Figure 2d; Hall et al., 2017) obtained from the Site U1478A cores, which constrain the age of the three transition boundaries as 3.5–3.3, 1.1–0.9, and 0.2–0.1 Ma (Figure 2). Magnetic susceptibility is low in sediments older than 3.5 Ma, increases and becomes more variable between 3.3 and 1.0 Ma, and next returns to low and less variable values until 0.2–0.1 Ma, when a renewed slight increase is recorded (Figure 2d).

4.1. Plio-Pleistocene Formation of the Modern Limpopo River

Comparison of core heavy-mineral data with potential source regions indicates that the provenance signatures observed in sediments deposited through time at Site U1478A offshore of the Limpopo River mouth become progressively closer to modern Limpopo sediments (Figures 1b and 2). We thus infer that the Limpopo River system as we see it today developed recently during the Plio-Quaternary by progressive headward erosion. This relatively late formation of the modern Limpopo River is not inconsistent with the long-held view that the river has a history that goes back to the Cretaceous (Du Toit, 1927; Moore & Larkin, 2001), but that our new analysis provides much more detailed information about the initiation of the modern river system, as we see it today.
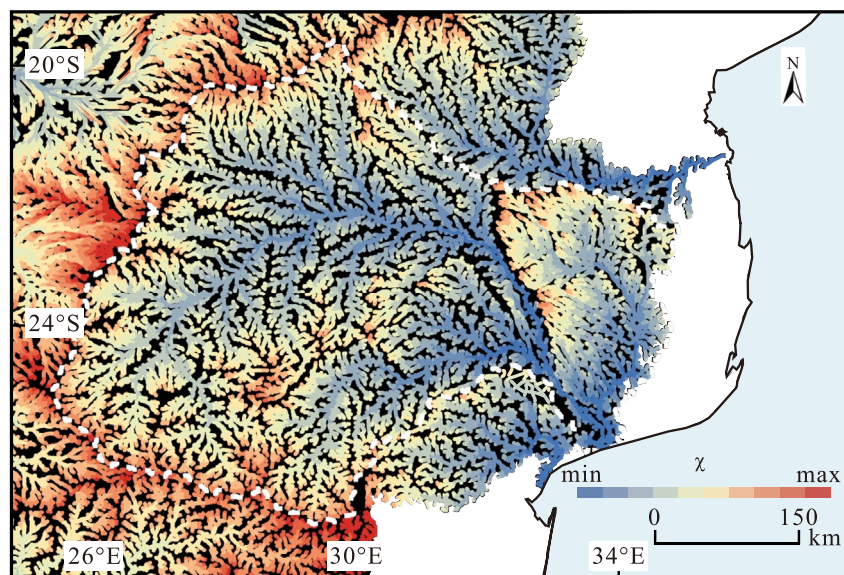

Figure 4. Map of χ values for the Limpopo River basin and its adjacent river networks. The lower χ values in the Limpopo drainage, compared to those neighboring drainages (drainage divide shown as dashed white line), indicate that the Limpopo River is expanding westward.

Marine sediments recovered during IODP Expedition 361 are not older than the Pliocene. Therefore, our data are unable to reconstruct the prior evolution of the river but do indicate that the provenance of the studied marine sediments changed significantly after 4 Ma. Furthermore, the different χ values between the Limpopo and its adjacent catchments show that the Limpopo River is far from being in equilibrium and is progressively expanding toward the west (Figure 4). Both lines of evidence suggest that the proto-Limpopo River was notably different from the modern river.

While this inferred Plio-Quaternary formation of the modern Limpopo River complements the long-held view that the river has a history that goes back to the Cretaceous (Du Toit, 1927; Moore & Larkin, 2001), it suggests that the classic model of the Limpopo-Zambezi river system evolution (e.g., Moore, 1988; Moore & Larkin, 2001) may have only partially considered all possible forcing mechanisms.

4.2. Accelerated River Formation Linked to Climatic Forcing

The current Limpopo River is sourced from the southern Africa Plateau at an elevation >1,000 m a.s.l. (Bond, 1979, Figure 1a). Different timings have been proposed regarding plateau uplift: Early Cretaceous (Gallagher & Brown, 1999; van der Beek et al., 2002), Late Cretaceous (Braun et al., 2014; Brown et al., 2002; de Wit, 2007; Flowers & Schoene, 2010; Tinker et al., 2008), Oligocene (Burke, 1996; Burke & Gunnel, 2008), and Plio-Quaternary (Partridge & Maud, 1987).

The currently available published data and resulting interpretations support the Late Cretaceous uplift, do not contradict the Oligocene uplift, but refute Plio-Quaternary uplift. First, thermochronological analysis and numerical models of escarpment erosion and retreat suggest that plateau uplift may have taken place as early as the Early Cretaceous (Gallagher & Brown, 1999; van der Beek et al., 2002). Second, thermochronological (Flowers & Schoene, 2010) and sedimentary flux data (Baby et al., 2020; Braun et al., 2014) from the continental margins of southern Africa support enhanced erosion of the plateau in the Late Cretaceous. Third, the Zambezi delta (Walford et al., 2005) and the South Mozambique Basin (Said et al., 2015) document rapid increase in sediment accumulation rate in the Oligocene and Miocene, respectively, at times when thermochronological data do not indicate accelerated exhumation. Particularly, apatite (U-Th)/He analysis (Flowers & Schoene, 2010) constrains Cenozoic exhumation as <850 m, which is consistent with the limited thickness of Cenozoic strata in the Zululand Basin (i.e., southernmost part of the South Mozambique Basin) (McMillan, 2003). Lastly, the Pliocene uplift of the southern Africa Plateau was proposed based purely on geomorphological evidence and it is not supported by an increase of sediment accumulation in surrounding basins (Moore & Blenkinsop, 2002). We conclude that there is no solid evidence supporting significant uplift of the southern Africa Plateau surface in our study area since the Pliocene.

The formation of the modern Limpopo River during the Plio-Pleistocene in an area lacking contemporaneous tectonic uplift suggests dominant climatic control on this recent evolution of the river. The first provenance shift documented in this study coincides in timing with climate wetting recorded by the leaf wax carbon-isotope record of ODP Site 1085 and the leaf wax hydrogen-isotope record of IODP Site 1478 (Figures 1a and 2; Maslin et al., 2012; Taylor et al., 2021). At ca. 3.3 Ma, the leaf wax carbon-isotope record of ODP Site 1085 shows a 2‰ decrease, indicating C_3 plant expansion and increasing humidity across the southern African continent (Figure 2b; Maslin et al., 2012). The leaf wax hydrogen-isotope record at IODP Site 1478 also shows progressively more negative δD_{wax} values, consistent with the carbon-isotope data from ODP Site 1085 (Figure 2c; Taylor et al., 2021). Together, this suggests that Late Pliocene climate change on the southern African continent may have promoted headwater erosion of the Limpopo River. The second shift recorded at ca. 1 Ma is not associated with the leaf wax carbon and hydrogen-isotope change but corresponds broadly to the onset of the Middle Pleistocene revolution, during which the dominant frequency of glacial-interglacial cyclicity changed from obliquity to 100-kyr eccentricity cycles with enhanced climatic fluctuations (Lisiecki & Raymo, 2005, Figure 2a). Many studies show that fluvial incision tends to occur during glacial-interglacial transitions (e.g., Pan et al., 2003; X. Wang et al., 2017; Zhang et al., 2001). Drainage-area expansion of the Limpopo River may have been associated with this climatic forcing. Larger-scale climate oscillations after the Middle Pleistocene revolution, whether during the last glacial-interglacial cycle or other glacial-interglacial cycles, led to enhanced stream power and hence more efficient headward erosion of the river. There is no record showing that either global or southern African climate experienced a significant shift at 0.2–0.1 Ma. Therefore, we attribute the incorporation of the upper Limpopo reaches

around 0.1 Ma as a result of the autogenic process of headward erosion. Because at least two samples show similar heavy-mineral assemblages for different stages during the Quaternary, it is unlikely that the documented compositional changes were caused by exceptional river floods rather than with evolution of regular drainage feeding annual flows.

A first-order minimum estimate of headward erosion can be gained from dividing the length of the Limpopo River between the site of sample #48 and the mouth by the age when the lower Limpopo River signal started to appear in strata of Site U1478A. This estimate amounts to 295 km Myr^{-1} (Figure S3a). A similar headward-erosion rate was calculated for the upper Yellow River during the Quaternary (350 km Myr^{-1}) (Craddock et al., 2010). Because the Limpopo River drains a stable cratonic block (Burke & Gunnel, 2008) whereas the upper Yellow River developed in a mobile compressional setting (Nie et al., 2015), such a similar headward-erosion rate in two different tectonic settings is consistent with the hypothesis that Plio-Pleistocene climate change represented the common forcing for drainage-area expansion.

During the Plio-Pleistocene, rapid drainage-area expansion or major changes in river courses are also observed in other large river systems in Africa (e.g., Zambezi River, Walford et al., 2005), Asia (e.g., Yangtze River, Fan & Li, 2008 and Jia et al., 2010), and worldwide (e.g., Rhine River, Boenigk & Frechen, 2006; Mississippi River, Hay et al., 1989). This consistency suggests that these drainage changes may have been all at least partly controlled by Plio-Pleistocene climate change, and specifically by the enhanced amplitude of climatic fluctuations (Lisiecki & Raymo, 2005) that promoted river incision and integration, and modified fluvial geomorphology over much of the Earth's surface.

Conflict of Interest

The authors declare no conflicts of interest relevant to this study.

Data Availability Statement

Supplementary figures can be found as part of the Supporting Information. Data obtained during this research can be downloaded from the figshare website (available at https://doi.org/10.6084/m9.figshare.13726693).

References

Aitchison, J. (1983). Principal component analysis of compositional data. *Biometrika*, *70*(1), 57–65. https://doi.org/10.1093/biomet/70.1.57

Aitchison, J., & Greenacre, M. (2002). Biplots of compositional data. *Journal of the Royal Statistical Society: Series C (Applied Statistics)*, *51*(4), 375–392. https://doi.org/10.1111/1467-9876.00275

Andò, S., & Garzanti, E. (2014). Raman spectroscopy in heavy-mineral studies. *Geological Society, London, Special Publications*, *386*(1), 395–412. https://doi.org/10.1144/SP386.2

Baby, G., Guillocheau, F., Braun, J., Robin, C., & Dall'Asta, M. (2020). Solid sedimentation rates history of the Southern African continental margins: Implications for the uplift history of the South African Plateau. *Terra Nova*, *32*(1), 53–65. https://doi.org/10.1111/ter.12435

Blum, M., Rogers, K., Gleason, J., Najman, Y., Cruz, J., & Fox, L. (2018). Allogenic and autogenic signals in the stratigraphic record of the Deep-Sea Bengal Fan. *Scientific Reports*, *8*(1), 7973. https://doi.org/10.1038/s41598-018-25819-5

Boenigk, W., & Frechen, M. (2006). The Pliocene and Quaternary fluvial archives of the Rhine system. *Quaternary Science Reviews*, *25*(5–6), 550–574. https://doi.org/10.1016/j.quascirev.2005.01.018

Bond, G. C. (1979). Evidence for some uplifts of large magnitude in continental platforms. *Tectonophysics*, *61*(1-3), 285–305. https://doi.org/10.1016/0040-1951(79)90302-0

Braun, J., Guillocheau, F., Robin, C., Baby, G., & Jelsma, H. (2014). Rapid erosion of the Southern African Plateau as it climbs over a mantle superswell. *Journal of Geophysical Research: Solid Earth*, *119*(7), 6093–6112. https://doi.org/10.1002/2014JB010998

Brown, R. W., Summerfield, M. A., & Gleadow, A. J. W. (2002). Denudational history along a transect across the Drakensberg Escarpment of Southern Africa derived from apatite fission track thermochronology. *Journal of Geophysical Research*, *107*(B12), ETG101-–ETG1018. https://doi.org/10.1029/2001JB000745

Burke, K. (1996). The African Plate. *South African Journal of Geology*, *99*(4), 341–409.

Burke, K., & Gunnel, Y. (2008). *The African erosion surface: A continental-scale synthesis of geomorphology, tectonics, and environmental change over the past 180 million years*. Memoir of the Geological Society of America. https://doi.org/10.1130/2008.1201

Cox, K. G. (1989). The role of mantle plumes in the development of continental drainage patterns. *Nature*, *342*, 873–877. https://doi.org/10.1038/342873a0

Craddock, W. H., Kirby, E., Harkins, N. W., Zhang, H., Shi, X., & Liu, J. (2010). Rapid fluvial incision along the Yellow River during headward basin integration. *Nature Geoscience*, *3*(3), 209–213. https://doi.org/10.1038/ngeo777

de Wit, M. C. J. (1999). Post-Gondwana drainage and the development of diamond placers in western South Africa. *Economic Geology*, *94*(5), 721–740. https://doi.org/10.2113/gsecongeo.94.5.721

de Wit, M. C. J. (2007). The Kalahari Epeirogeny and climate change: Differentiating cause and effect from core to space. *South African Journal of Geology*, *110*(2–3), 367–392. https://doi.org/10.2113/gssajg.110.2-3.367

Du Toit, A. L. (1927). The Kalahari and some of its problems. *South African Journal of Science*, *24*, 88–101.

Fan, D., & Li, C. (2008). Timing of the Yangtze initiation draining the Tibetan Plateau throughout to the East China Sea: A review. *Frontiers of Earth Science in China*, *2*(3), 302–313. https://doi.org/10.1007/s11707-008-0018-9

Flowers, R. M., & Schoene, B. (2010). U-Th)/He thermochronometry constraints on unroofing of the eastern Kaapvaal craton and significance for uplift of the southern African Plateau. *Geology*, *38*(9), 827–830. https://doi.org/10.1130/G30980.1

Gallagher, K., & Brown, R. (1999). Denudation and uplift at passive margins: The record on the Atlantic Margin of southern Africa. *Philosophical Transactions of the Royal Society of London, Series A: Mathematical, Physical and Engineering Sciences*, *357*(1753), 835–859. https://doi.org/10.1098/rsta.1999.0354

Galy, V., France-Lanord, C., Beyssac, O., Faure, P., Kudrass, H., & Palhol, F. (2007). Efficient organic carbon burial in the Bengal fan sustained by the Himalayan erosional system. *Nature*, *450*(7168), 407–410. https://doi.org/10.1038/nature06273

Garzanti, E. (2016). From static to dynamic provenance analysis—Sedimentary petrology upgraded. *Sedimentary Geology*, *336*, 3–13. https://doi.org/10.1016/j.sedgeo.2015.07.010

Garzanti, E., & Andò, S. (2019). Heavy minerals for junior Woodchucks. *Minerals*, *9*(3), 148. https://doi.org/10.3390/min9030148

Garzanti, E., Vermeesch, P., Padoan, M., Resentini, A., Vezzoli, G., & Andò, S. (2014). Provenance of passive-margin sand (Southern Africa). *The Journal of Geology*, *122*(1), 17–42. https://doi.org/10.1086/674803

Greenacre, M. (1984). *Theory and applications of correspondence analysis* (p. 364). Academic Press.

Hahn, A., Miller, C., Andò, S., Bouimetarhan, I., Cawthra, H. C., Garzanti, E., et al. (2018). The provenance of terrigenous components in marine sediments along the east coast of Southern Africa. *Geochemistry, Geophysics, Geosystems*, *19*(7), 1946–1962. https://doi.org/10.1029/2017GC007228

Hall, I. R., Hemming, S. R., LeVay, L. J., Barker, S., Berke, M. A., Brentegani, L., et al. (2017). Site U1478. *Proceedings of the International Ocean Discovery Program*, *361*. Retrieved from http://www.researchgate.net/publication/320133056_Site_U1478

Hällberg, L. P., Stevens, T., Almqvist, B., Snowball, I., Wiers, S., Költringer, C., et al. (2020). Magnetic susceptibility parameters as proxies for desert sediment provenance. *Aeolian Research*, *46*, 100615. https://doi.org/10.1016/j.aeolia.2020.100615

Hay, W. W., Shaw, C. A., & Wold, C. N. (1989). Mass-balanced paleogeographic reconstructions. *Geologische Rundschau*, *78*(1), 207–242. https://doi.org/10.1007/BF01988362

Jia, J., Zheng, H., Huang, X., Wu, F., Yang, S., Wang, K., & He, M. (2010). Detrital zircon U-Pb ages of Late Cenozoic sediments from the Yangtze delta: Implication for the evolution of the Yangtze River. *Chinese Science Bulletin*, *55*(15), 1520–1528. https://doi.org/10.1007/s11434-010-3091-x

Jonell, T. N., Carter, A., Böning, P., Pahnke, K., & Clift, P. D. (2017). Climatic and glacial impact on erosion patterns and sediment provenance in the Himalayan rain shadow, Zanskar River, NW India. *The Geological Society of America Bulletin*, *129*(7–8), 820–836. https://doi.org/10.1130/B31573.1

Key, R. M., Cotterill, F. P. D., & Moore, A. E. (2015). The Zambezi River: An archive of tectonic events linked to the amalgamation and disruption of Gondwana and subsequent evolution of the African Plate. *South African Journal of Geology*, *118*(4), 425–438. https://doi.org/10.2113/gssajg.118.4.425

Koutsodendris, A., Nakajima, K., Kaboth-Bahr, S., Berke, M. A., Franzese, A. M., Hall, I. R., et al. (2021). A Plio-Pleistocene (c. 0–4 Ma) cyclostratigraphy for IODP Site U1478 (Mozambique Channel, SW Indian Ocean): Exploring an offshore record of paleoclimate and ecosystem variability in SE Africa. *Newsletters on Stratigraphy*, *54*(2), 159–181. https://doi.org/10.1127/nos/2020/0608

Li, J., Fang, X., Song, C., Pan, B., Ma, Y., & Yan, M. (2014). Late Miocene–Quaternary rapid stepwise uplift of the NE Tibetan Plateau and its effects on climatic and environmental changes. *Quaternary Research*, *81*(3), 400–423. https://doi.org/10.1016/j.yqres.2014.01.002

Lisiecki, L. E., & Raymo, M. E. (2005). A Pliocene-Pleistocene stack of 57 globally distributed benthic δ18O records. *Paleoceanography*, *20*(1), PA1003. https://doi.org/10.1029/2004PA001071

Maher, B. A. (2011). The magnetic properties of Quaternary aeolian dusts and sediments, and their palaeoclimatic significance. *Aeolian Research*, *3*(2), 87–144. https://doi.org/10.1016/j.aeolia.2011.01.005

Maslin, M. A., Pancost, R. D., Wilson, K. E., Lewis, J., & Trauth, M. H. (2012). Three and half million year history of moisture availability of South West Africa: Evidence from ODP site 1085 biomarker records. *Palaeogeography, Palaeoclimatology, Palaeoecology*, *317–318*, 41–47. https://doi.org/10.1016/j.palaeo.2011.12.009

McMillan, I. K. (2003). Foraminiferally defined bilostratigraphic episodes and sedimentation pattern of the Cretaceous drift succession (Early Barremian to Late Maastrichtian) in seven basins on the South African and southern Namibian continental margin. *South African Journal of Science*, *99*(11–12), 537–576.

Moore, A. E. (1988). Plant distribution and the evolution of the major river systems in southern Africa. *South African Journal of Geology*, *91*, 346–349.

Moore, A. E., & Blenkinsop, T. (2002). The role of mantle plumes in the development of continental-scale drainage patterns: The southern African example revisited. *South African Journal of Geology*, *105*(4), 353–360. https://doi.org/10.2113/1050353

Moore, A. E., Blenkinsop, T., & Cotterill, F. (2009). Southern African topography and erosion history: Plumes or plate tectonics? *Terra Nova*, *21*(4), 310–315. https://doi.org/10.1111/j.1365-3121.2009.00887.x

Moore, A. E., & Larkin, P. A. (2001). Drainage evolution in south-central Africa since the breakup of Gondwana. *South African Journal of Geology*, *104*(1), 47–68. https://doi.org/10.2113/104.1.47

Moucha, R., & Forte, A. M. (2011). Changes in African topography driven by mantle convection. *Nature Geoscience*, *4*(10), 707–712. https://doi.org/10.1038/ngeo1235

Nie, J., Horton, B. K., Saylor, J. E., Mora, A., Mange, M., Garzione, C. N., et al. (2012). Integrated provenance analysis of a convergent retroarc foreland system: U–Pb ages, heavy minerals, Nd isotopes, and sandstone compositions of the Middle Magdalena Valley basin, northern Andes, Colombia. *Earth-Science Reviews*, *110*(1–4), 111–126. https://doi.org/10.1016/j.earscirev.2011.11.002

Nie, J., Stevens, T., Rittner, M., Stockli, D., Garzanti, E., Limonta, M., et al. (2015). Loess Plateau storage of Northeastern Tibetan Plateau-derived Yellow River sediment. *Nature Communications*, *6*, 8511. https://doi.org/10.1038/ncomms9511

Pan, B., Burbank, D., Wang, Y., Wu, G., Li, J., & Guan, Q. (2003). A 900 k.y. record of strath terrace formation during glacial-interglacial transitions in northwest China. *Geology*, *31*(11), 957–960. https://doi.org/10.1130/G19685.1

Partridge, T. C., & Maud, R. R. (1987). Geomorphic evolution of southern Africa since the Mesozoic. *South African Journal of Geology*, *90*, 179–208.

Perron, J. T., & Royden, L. (2013). An integral approach to bedrock river profile analysis. *Earth Surface Processes and Landforms*, *38*(6), 570–576. https://doi.org/10.1002/esp.3302

Said, A., Moder, C., Clark, S., & Ghorbal, B. (2015). Cretaceous–Cenozoic sedimentary budgets of the Southern Mozambique Basin: Implications for uplift history of the South African Plateau. *Journal of African Earth Sciences*, *109*, 1–10. https://doi.org/10.1016/j.jafrearsci.2015.05.007

Schüürman, J., Hahn, A., & Zabel, M. (2019). In search of sediment deposits from the Limpopo (Delagoa Bight, southern Africa): Deciphering the catchment provenance of coastal sediments. *Sedimentary Geology*, *380*, 94–104. https://doi.org/10.1016/j.sedgeo.2018.11.012

Spaliviero, M., De Dapper, M., & Maló, S. (2014). Flood analysis of the Limpopo River basin through past evolution reconstruction and a geomorphological approach. *Natural Hazards and Earth System Sciences*, *14*(8), 2027–2039. https://doi.org/10.5194/nhess-14-2027-2014

Taylor, A. K., Berke, M. A., Castañeda, I. S., Koutsodendris, A., Campos, H., Hall, I. R., et al. (2021). Plio-Pleistocene continental hydroclimate and Indian Ocean sea surface temperatures at the Southeast African margin. *Paleoceanography and Paleoclimatology*, *36*(3). https://doi.org/10.1029/2020pa004186

Tinker, J., de Wit, M., & Brown, R. (2008). Mesozoic exhumation of the southern Cape, South Africa, quantified using apatite fission track thermochronology. *Tectonophysics*, *455*(1–4), 77–93. https://doi.org/10.1016/j.tecto.2007.10.009

van der Beek, P., Summerfield, M. A., Braun, J., Brown, R. W., & Fleming, A. (2002). Modeling postbreakup landscape development and denudational history across the southeast African (Drakensberg Escarpment) margin. *Journal of Geophysical Research*, *107*(B12). https://doi.org/10.1029/2001JB000744

Vermeesch, P. (2018). Statistical models for point-counting data. *Earth and Planetary Science Letters*, *501*, 112–118. https://doi.org/10.1016/j.epsl.2018.08.019

Vermeesch, P., Resentini, A., & Garzanti, E. (2016). An R package for statistical provenance analysis. *Sedimentary Geology*, *336*, 14–25. https://doi.org/10.1016/j.sedgeo.2016.01.009

Walford, H., White, N., & Sydow, J. (2005). Solid sediment load history of the Zambezi Delta. *Earth and Planetary Science Letters*, *238*(1–2), 49–63. https://doi.org/10.1016/j.epsl.2005.07.014

Wang, X., Vandenberghe, J., Lu, H., & van Balen, R. (2017). Climatic and tectonic controls on the fluvial morphology of the Northeastern Tibetan Plateau (China). *Journal of Geographical Sciences*, *27*(11), 1325–1340. https://doi.org/10.1007/s11442-017-0000-0

Wang, Z., Nie, J., Wang, J., Zhang, H., Peng, W., Garzanti, E., et al. (2019). Testing contrasting models of the formation of the upper Yellow river using heavy-mineral data from the Yinchuan basin drill cores. *Geophysical Research Letters*, *46*(17–18), 10338–10345. https://doi.org/10.1029/2019GL084179

Willett, S. D., McCoy, S. W., Perron, J. T., Goren, L., & Chen, C. Y. (2014). Dynamic reorganization of river basins. *Science*, *343*, 1248765 https://doi.org/10.1126/science.1248765

Zhang, P., Molnar, P., & Downs, W. R. (2001). Increased sedimentation rates and grain sizes 2-4 Myr ago due to the influence of climate change on erosion rates. *Nature*, *410*, 891–897. https://doi.org/10.1038/35073504

Zheng, H., Clift, P. D., Wang, P., Tada, R., Jia, J., He, M., & Jourdan, F. (2013). Pre-Miocene birth of the Yangtze River. *Proceedings of the National Academy of Sciences of the United States of America*, *110*(19), 7556–7561. https://doi.org/10.1073/pnas.1216241110

References From the Supporting Information

Ferrier, K. L., Huppert, K. L., & Perron, J. T. (2013). Climatic control of bedrock river incision. *Nature*, *496*(7444), 206–209. https://doi.org/10.1038/nature11982

Vermeesch, P. (2012). On the visualisation of detrital age distributions. *Chemical Geology*, *312–313*, 190–194. https://doi.org/10.1016/j.chemgeo.2012.04.021